Ground-State Quasirotational Bands to 8^+ in $^{114-126}$Te Produced by (α, xn)†

R. A. WARNER* AND J. E. DRAPER
Crocker Nuclear Laboratory,‡ University of California, Davis, California 95616
(Received 24 September 1969)

Measurements of the γ spectra, time distributions, angular distributions, and excitation functions of γ rays from $(\alpha, 2n)$ and $(\alpha, 4n)$ reactions producing the vibrators $^{114-126}$Te reveal that the most prominent γ rays are in $8^+\rightarrow6^+\rightarrow4^+\rightarrow2^+\rightarrow0^+$ cascades. The energies and intensities exhibit remarkably regular systematics.

I. INTRODUCTION

IN-BEAM spectroscopy with (α, xn) and (HI, xn) reactions and more conventional spectroscopy have revealed a remarkably regular pattern of quasirotational ground-state bands in a large fraction of all even-even[1,2] nuclei of mass greater than about 70. Our study of the eight even-even nuclei $^{112-126}$Te was motivated by their lying along the edge of a proposed[3] region of deformation and by the question whether the Te nuclei would exhibit a pattern of levels similar to those already mentioned above when Te is only two protons removed from a closed shell and therefore is usually regarded as a vibrator. Other studies of Te nuclei by (α, xn) have been made,[4–7] but they are incomplete and present conflicting results. The preliminary Te results in Bergström *et al.*[6] are described in one paragraph of that article on Xe.

II. SOME FEATURES OF THE REACTION MECHANISM

The mechanism of these reactions has been investigated by several authors.[8–10] In order to augment their work, we summarize the results of a calculation of the probability distribution for the angular momentum of the compound nucleus. In addition, we briefly review the features of the deexcitation which are pertinent to the experiment.

First we calculate, following Huizenga and Igo,[11] the reaction cross section for α particles as

$$\sigma_R{}^l=\pi\lambda\!\!\!^{-2}(2l+1)T_l, \tag{1}$$

where T_l is the transmission coefficient for the partial wave l through the barrier. The barrier is approximated by a parabola for which, after correction of a typographical error in Ref. 11, we have

$$T_l=\{1+\exp[-2\pi(E-B_l)/\hbar\omega_l]\}^{-1}, \tag{2}$$

where B_l is the barrier height and

$$\hbar\omega_l=\left|\frac{\hbar^2}{\mu}\frac{d^2V_l}{dr^2}\right|^{1/2} \tag{3}$$

evaluated at the maximum of the potential

$$V_l=\frac{2Ze^2}{r}+\frac{l(l+1)\hbar^2}{2\mu r^2}-1100\text{ MeV}\times\exp\left(-\frac{r-1.17A^{1/3}}{0.574\text{ fm}}\right). \tag{4}$$

The constants are those of Huizenga and Igo.[11] The resulting reaction cross section for producing the compound state is shown in Fig. 1 for conditions typical of the present experiment.

Figure 1 shows that for 70-MeV α particles there is significant cross section for $\lesssim 28$ units of angular momentum. For even-even targets this angular momentum is aligned with only $M=0$ with respect to the direction of the α beam. In (α, xn) reactions the evaporated neutrons carry away about $10x$ MeV but little angular momentum. The succeeding early γ rays quickly cascade ($\lesssim 10^{-11}$ sec) to the YRAST levels[8,10] and to the ground-state band producing many unresolved γ rays. The angular momentum is still strongly aligned upon entrance into the ground-state band.

Experimentally, the prominent features of the γ-ray spectra from medium-weight nuclei measured with resolution of 2–4 keV are mostly the transitions within the ground-state band. Since the angular momentum is still strongly aligned, the angular distribution of the

† Much of this material is derived from a thesis submitted by R.A.W. in partial fulfillment of the requirements for the Ph.D.
‡ Supported in part by the U.S. Atomic Energy Commission.
* Present address: Michigan State University Cyclotron, Michigan State University, East Lansing, Mich. 48823.

[1] M. A. J. Mariscotti, G. Scharff-Goldhaber, and B. Buck, Phys. Rev. **178**, 1864 (1969).
[2] J. E. Draper, D. G. McCauley, and G. L. Smith (to be published).
[3] E. Marshalek, L. W. Person, and R. K. Sheline, Rev. Mod. Phys. **35**, 108 (1963).
[4] H. Ejiri, M. Ishihara, M. Sakai, T. Inamura, and K. Katori, J. Phys. Soc. Japan **21**, 1 (1966).
[5] M. G. Betigeri and H. Morinaga, Nucl. Phys. **A95**, 176 (1967).
[6] I. Bergström, C. J. Herrlander, A. Kerek, and A. Luukko, Nucl. Phys. **A123**, 99 (1969a).
[7] R. A. Warner and J. E. Draper, Bull. Am. Phys. Soc. **14**, 490 (1969).
[8] J. R. Grover and J. Gilat, Phys. Rev. **157**, 814 (1967).
[9] I. Halpern, B. J. Shepherd, and C. F. Williamson, Phys. Rev. **169**, 805 (1968).
[10] J. O. Newton, F. S. Stephens, R. M. Diamond, W. H. Kelly, and D. Ward, University of California Lawrence Radiation Laboratory Report No. UCRL-18358 Rev, 1969 (to be published).
[11] J. R. Huizenga and G. Igo, Nucl. Phys. **29**, 462 (1962).

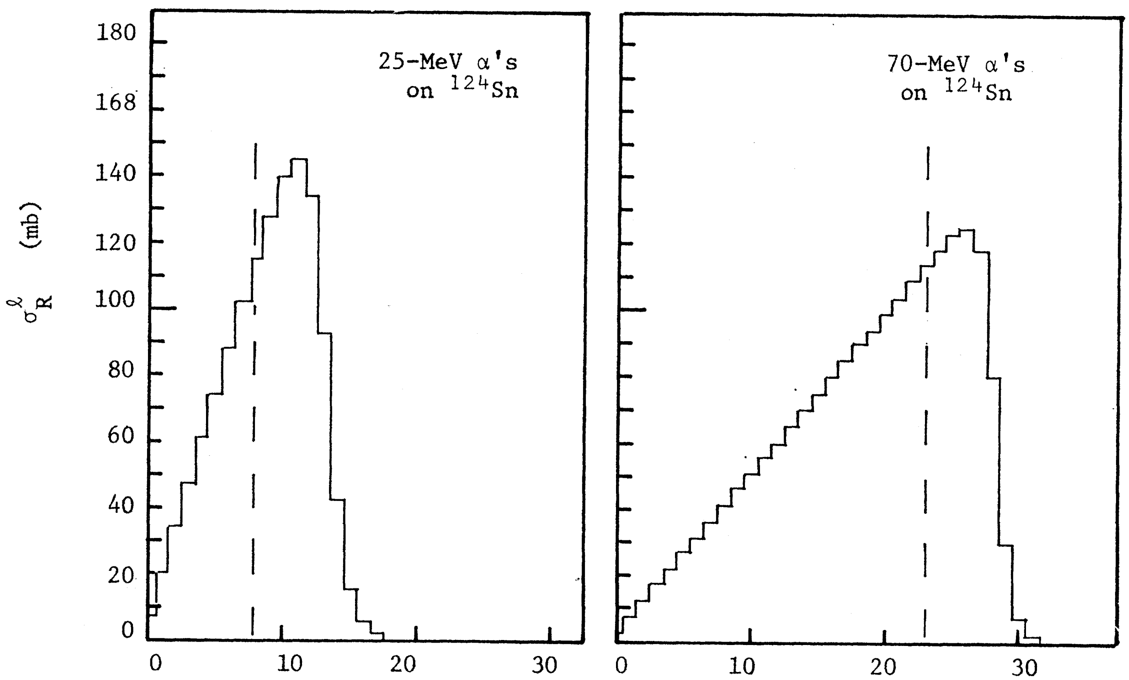

FIG. 1. Theoretical l dependence of the cross section for formation of a compound nucleus for 25-MeV and 70-MeV α particles on ^{124}Sn. The dashed line is the classical maximum orbital angular momentum evaluated at $1.17\ A^{1/3}+1.77$ fm.

γ rays is a powerful experimental tool for identification of the transitions, as first demonstrated by Williamson and Shepherd[12] and by Ejiri *et al.*[13]

III. EXPERIMENTAL METHOD

α-particle beams of 25–75 MeV were obtained from the Davis 76-in. AVF cyclotron. The cyclotron can be tuned so the natural beam bunches are <2.0 nsec full width at half-maximum. This is the total width of the curve obtained by measurement of the time of arrival of α particles elastically scattered into a plastic scintillator. The reference time zero is obtained from a thin plastic scintillator placed directly in the cyclotron beam[14] $\sim$50 cm downstream from the target. This thin scintillator has good longevity in the beams of 1–20 nA used in these experiments. The time spectrum shows that the sides of the peak are steep and that there are no counts between beam bursts.

This short duration of beam burst allowed us to measure half-lives of transitions from $\sim$3 to 200 nsec. In order to achieve this it was necessary to correct for "walk" [pulse-height dependence of the time of response of the trigger circuit to Ge(Li) pulses]. The "walk" was reduced from 11 to 3 nsec by appropriately mixing the TAC (time-to-amplitude converter) pulse with the logarithm of the Ge(Li) pulse height. With this correction the spectrum of TAC pulses [started by Ge(Li) and stopped by the downstream scintillator] was 6 nsec full width at half-maximum for all γ rays above a threshold of 100 keV.

Powder targets were typically 25 mg of separated isotopes of SnO_2 cemented with 2 mg/cm^2 of clear acrylic spray enamel to a 1-cm^2 spot on a strip of 0.00025 in. Mylar 4 mm wide. They were located in a scattering chamber which is also used in other experiments with a high resolution Si junction detector for conversion-electron spectra.

The Ge(Li) detector is planar for fast timing. It is of 6-mm depletion depth and 6 cm^2 in area. It is located 11 in. from the target, and its angular position can be varied remotely from 32° to 148° with respect to the α beam. Another Ge(Li) detector is fixed at a forward angle for beam monitoring during a measurement of angular distribution of the γ rays.

The spectra were analyzed in a TMC 4096-channel analyzer. For measurements of half-life, this is operated in eight bands of 512 channels of γ pulse height. The eight bands contain the time information from a digital sorter of the TAC pulses. The early time channels are often 5 nsec wide and the later channels are increasingly wide to cover, without gaps, the remainder of the $\sim$100 nsec period of the cyclotron dee voltage.

One of the most difficult problems in measuring these angular distributions with the cyclotron was the correction for dead time in the analyzer. The reason is that the cyclotron beam current on target often fluctuates repetitively by an order of magnitude during each period

[12] C. F. Williamson and B. J. Shepherd, Bull. Am. Phys. Soc. **10**, 428 (1965).
[13] H. Ejiri, M. Ishihara, M. Sakai, K. Katori, and T. Inamura, Phys. Letters **18**, 314 (1965).
[14] R. A. Warner, G. L. Smith, R. M. Lieder, and J. E. Draper, Nucl. Instr. Method **75**, 149 (1969).

of 60 Hz (the frequency of power mains). This fine structure (characteristic period ~0.1 to 10 msec) as well as the average beam current vary with approximately half-hour periods. The resulting dead time in the analyzer does not distort a given purely prompt spectrum, but it makes difficult the quantitative comparison of counting rate from run to run as required for the angular distributions. The essential problem is that the analyzer dead time depends strongly on the half-life of the transition in question. In typical runs the dead-time meter registered 50% when the digital sorter was in use. Consequently, a brief analysis of the problem and its solution is presented in the Appendix, since the only alternative to this solution was to run at prohibitively low counting rate.

The transition intensities and angular distributions were evaluated as follows. Defining $I_{\gamma i}W_i(\theta)$ as the probability of emission of a γ ray from the ith transition at angle θ for transition probability $I_{\gamma i}$ and angular distribution $W_i(\theta)$, then

$$I_{\gamma i}W_i(\theta)=\text{const}C_i(\theta)/\langle r_{\text{trig}}\rangle L_i(\theta)\epsilon_i(\theta), \qquad (5)$$

where $C_i(\theta)$ is the number of counts recorded in the ith peak of the spectrum, $\langle r_{\text{trig}}\rangle$ is the average rate of generation of triggered pulses by the fixed monitor detector (proportional to reaction rate), L_i is given in Eq. (A1), and $\epsilon_i(\theta)$ is the product of the angle-dependent transmission of the γ rays i through the window of the scattering chamber and the angle-independent efficiency of the moveable detector for γ ray i. In the case that transition i has half-life$\ll$dead time T, this becomes

$$I_{\gamma i}W_i(\theta)=\text{const}C_i(\theta)/C_{\text{trig}}(\theta)\epsilon_i(\theta), \qquad (6)$$

where $C_{\text{trig}}(\theta)$ is the number of counts recorded in the triggered pulser peak. The approximate Eq. (6) could not be used in tests of roundness of the system with (α, xn) γ rays sufficiently long-lived that they were known to be isotropic.

IV. EXPERIMENTAL RESULTS

A. Pulse-Height Spectra

Figures 2(a) and 2(b) are two-parameter spectra in pulse height and time. Although such spectra were accumulated for $(\alpha, 2n)$, $(\alpha, 3n)$, and $(\alpha, 4n)$ reactions on all the stable Sn isotopes, we show only spectra where ^{126}Te and ^{120}Te were produced, to conserve journal space and yet display examples of transitions with both prompt and delayed feeding [Fig. 2(a)] and transitions fed only promptly [Fig. 2(b)].

Some features recur in the spectra of Figs. 2 and 3. The broad peaks labeled N at about 695 keV result from $E0$ deexcitation of the 290-nsec 690-keV state[15] in ^{72}Ge from ^{72}Ge(n, n') in the detector. Their breadth is caused by the variable time of summing of the pulses from the recoil energy of the ^{72}Ge and from the conversion electrons. Transitions at 110, 184, 197, and 937 keV result from reactions with oxygen in the target. A line at 238 keV common to reactions at low α energies has not been identified. Some spectra contain lines at 843 and 1013 keV which are only in a later band or two. These are caused by an aluminum obstruction sometimes present 16 nsec downstream from the target.

Energies underlined in Figs. 2 and 3 are those used in the level scheme of Fig. 7.

B. Time Distributions

Figure 4 shows examples of time distributions taken from data as in Fig. 2. Figure 4(a) shows the time distribution of prompt transitions in ^{114}Te. These and most of the other transitions given in the energy-level diagrams later had the same prompt distributions with measured half-lives $\lesssim$3 nsec for at least 90% of the transition intensity. The only exceptions are shown in Fig. 4(b), where all transitions have a 13-nsec delayed component, and only the 209-keV transition does not have a prompt component.

Time distributions of the 511-keV lines from various targets always show a prompt peak, probably caused by positrons from high-energy prompt γ rays. This renders meaningless their angular distribution.

Measured time distributions of the common transitions show the 110 keV in ^{19}F to be mostly prompt, the 184 keV in ^{18}F to be ~150 nsec and the 197 keV in ^{19}F to be ~87 nsec. The 238 keV is 18±2 nsec and the 937 keV in ^{18}F is 32% prompt and 68% with $\gtrsim$150-nsec half-life.

C. Angular Distributions

The angular distributions of the transitions in the ground-state bands are in Fig. 5. The data are fitted by the function

$$W(\theta)=A_0+A_2P_2(\cos\theta)+A_4P_4(\cos\theta), \qquad (7)$$

subject to normalization. The parameters used in calculating the curves of Fig. 5 are discussed in Sec. V. Data from other γ rays show a variety of distributions. None of the following transitions has an angular distribution similar to the characteristic stretched $E2$ shape of Fig. 5: the 926 keV in Fig. 2(b), the 297 keV in Fig. 2(a), the 720 keV in Fig. 2(a), the 856 keV in Fig. 2(a), and the 110- and 197-keV common transitions. The 238-keV common transition has an angular distribution somewhat like stretched $E2$. The 753-keV angular distribution of Figs. 2(a) and 3 is nearly isotropic and is consistent with its assignment to $2^{+\prime}\rightarrow 2^+$.

The distributions in the lower right-hand corner of Fig. 5 correspond to prompt transitions tentatively assigned to ^{126}Te, but not placed in the level scheme. These two distributions only are fitted with no theoret-

[15] C. M. Lederer, J. M. Hollander, and I. Perlman, *Table of Isotopes* (John Wiley & Sons, New York, 1967), 6th ed.

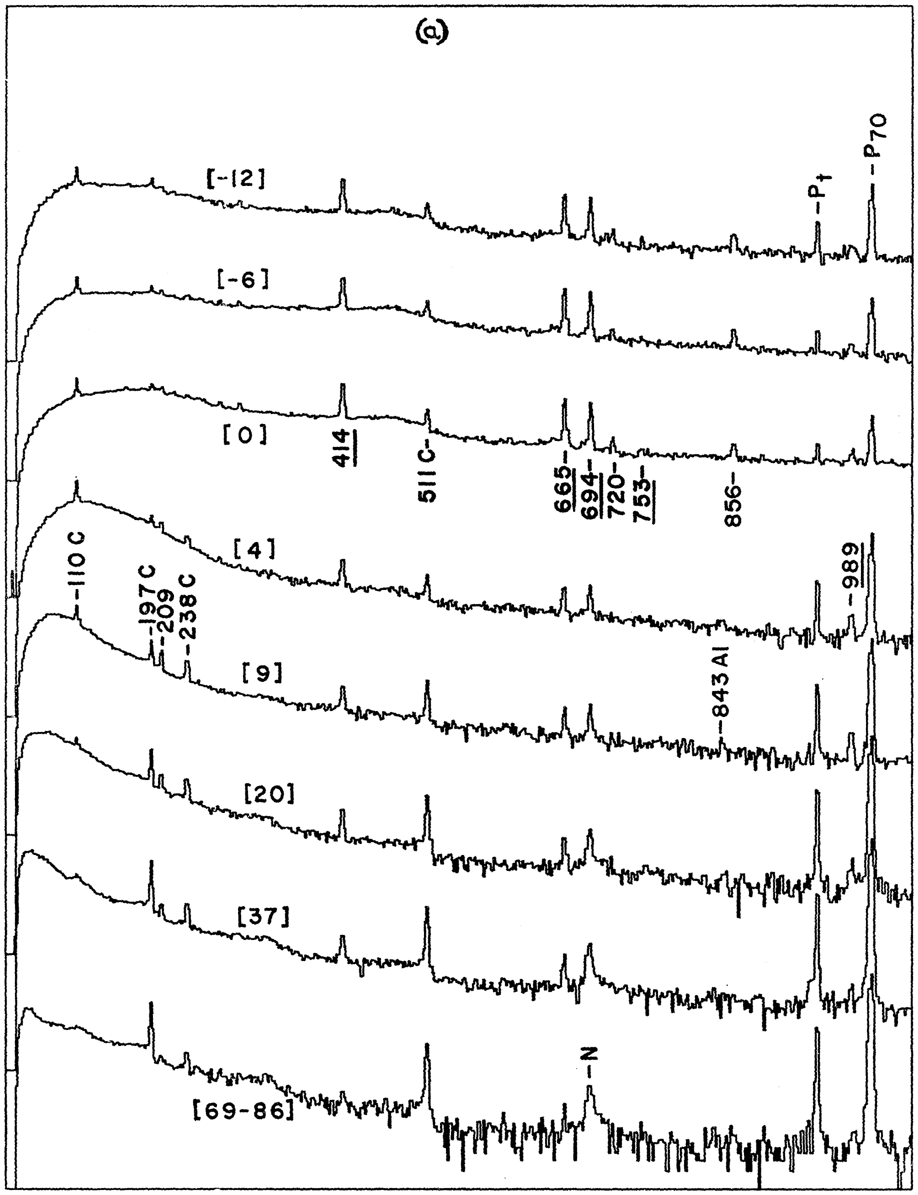

FIG. 2. (a) Time dependence of the γ-ray spectra from 25-MeV (α, $2n$) ^{126}Te. The peaks are labeled by energy (keV) and those appearing in Fig. 7 are underlined. The eight contiguous time bands are labeled with their time (nsec) of initiation with respect to the center of the α beam bunch. For example, the top band is 12 to 6 nsec before the beam; the bottom band is 69 to 86 nsec after the beam. The peaks labeled C are common to at least several targets as described in the text. Peak N is caused by fast neutrons in the Ge detector. The labels P_t and P_{70} denote the triggered pulser and 70-Hz pulser used for analyzer dead-time correction. The semilog spectra are separated by factors of 100. (b) 26-MeV (α, $2n$) ^{120}Te.

ical constraints on the values of A_0, A_2, and A_4 in Eq. (7).

D. Excitation Functions

For the purpose of *a priori* selection of optimum α energies the expression

$$E_\alpha^{\text{opt}} = -Q + 7x \text{ (MeV)} \tag{8}$$

was satisfactory for (α, xn) reactions. Here $-Q$ is the threshold for the reaction.

The dependence of the γ-ray yield on the α energy is important in isotopic identification of the transition. If only (α, $2n$) data were obtained, this identification would be much less certain because of possible contamination from (α, n), (α, $3n$), or target impurities. Consequently, we include (α, $4n$) data for each Te iso-

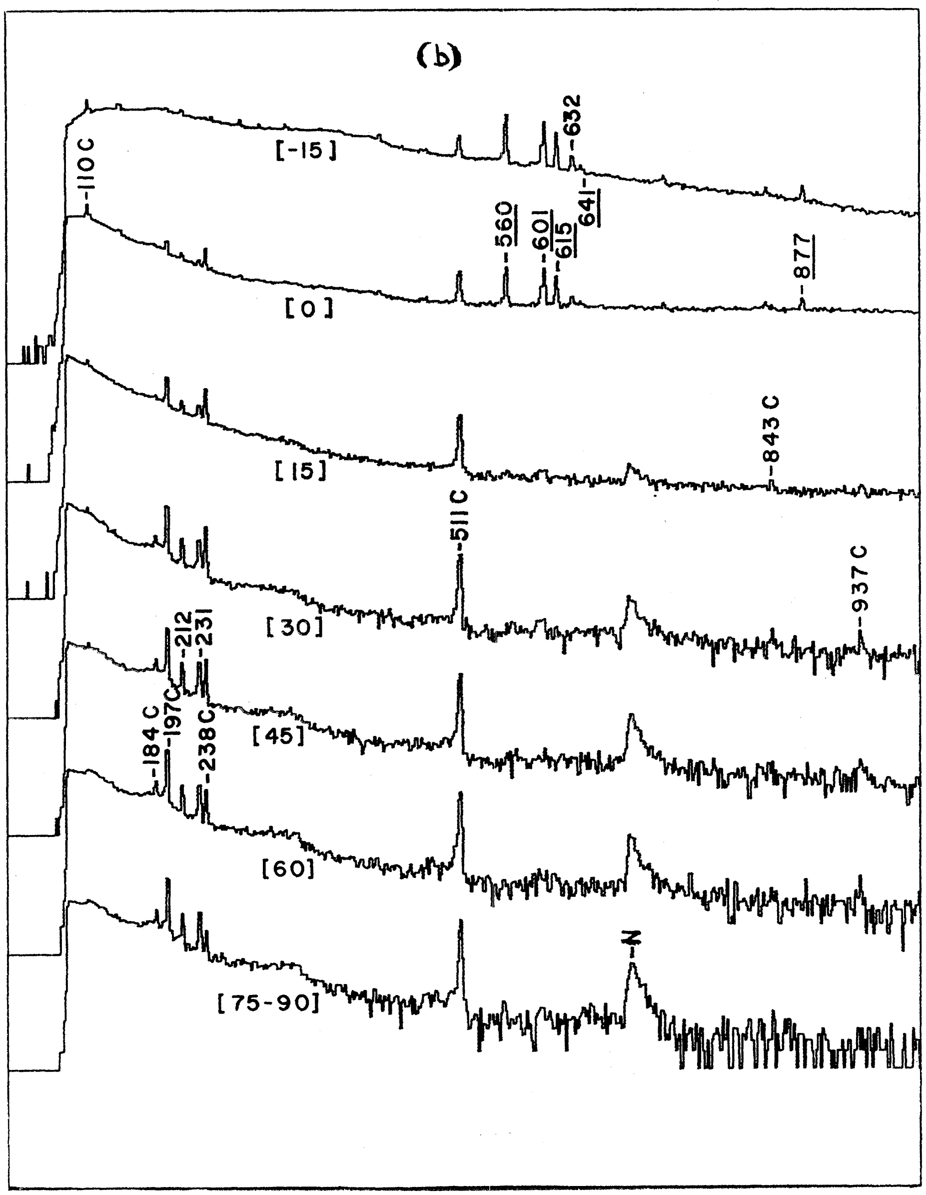

Fig. 2. (*Continued*).

tope, thus having data from two different target isotopes for each product isotope. Furthermore, it is of interest to determine empirically the extent to which the relative intensities of the transitions depend on the spin of the parent level as the beam energy is increased.

The dependence of the relative transition intensities on E_α is shown in Fig. 6 so that the general features may be visualized. One might expect that the relative intensities of transitions from the high-spin states would usually increase as the initial excitation energy of the residual nucleus. Figure 6 confirms this tendency, but it is not sufficiently pronounced (e.g., ^{126}Te and ^{118}Te) to serve as a reliable basis for spin assignments. One might have expected a larger difference between the $(\alpha, 2n)$ and $(\alpha, 4n)$ results in Fig. 6 with $(\alpha, 4n)$ intensities being more nearly equal. Note that the excitation energy is ~10 MeV for $(\alpha, 2n)$ and ~20 MeV for $(\alpha, 4n)$ assuming that each of the x neutrons in Eq. (8) carries away ~2 MeV of kinetic energy.

There was not sufficient space in Fig. 6 to include the experimental uncertainties in the relative intensities. The uncertainties are approximately 15% for strong $(\alpha, 2n)$ γ rays and approximately 25% for $(\alpha, 4n)$ γ rays. The apparent discrepancy of the relative intensity of the $4^+ \rightarrow 2^+$ transition compared to the $2^+ \rightarrow 0^+$ for ^{118}Te at 62 MeV is within these errors. The similar

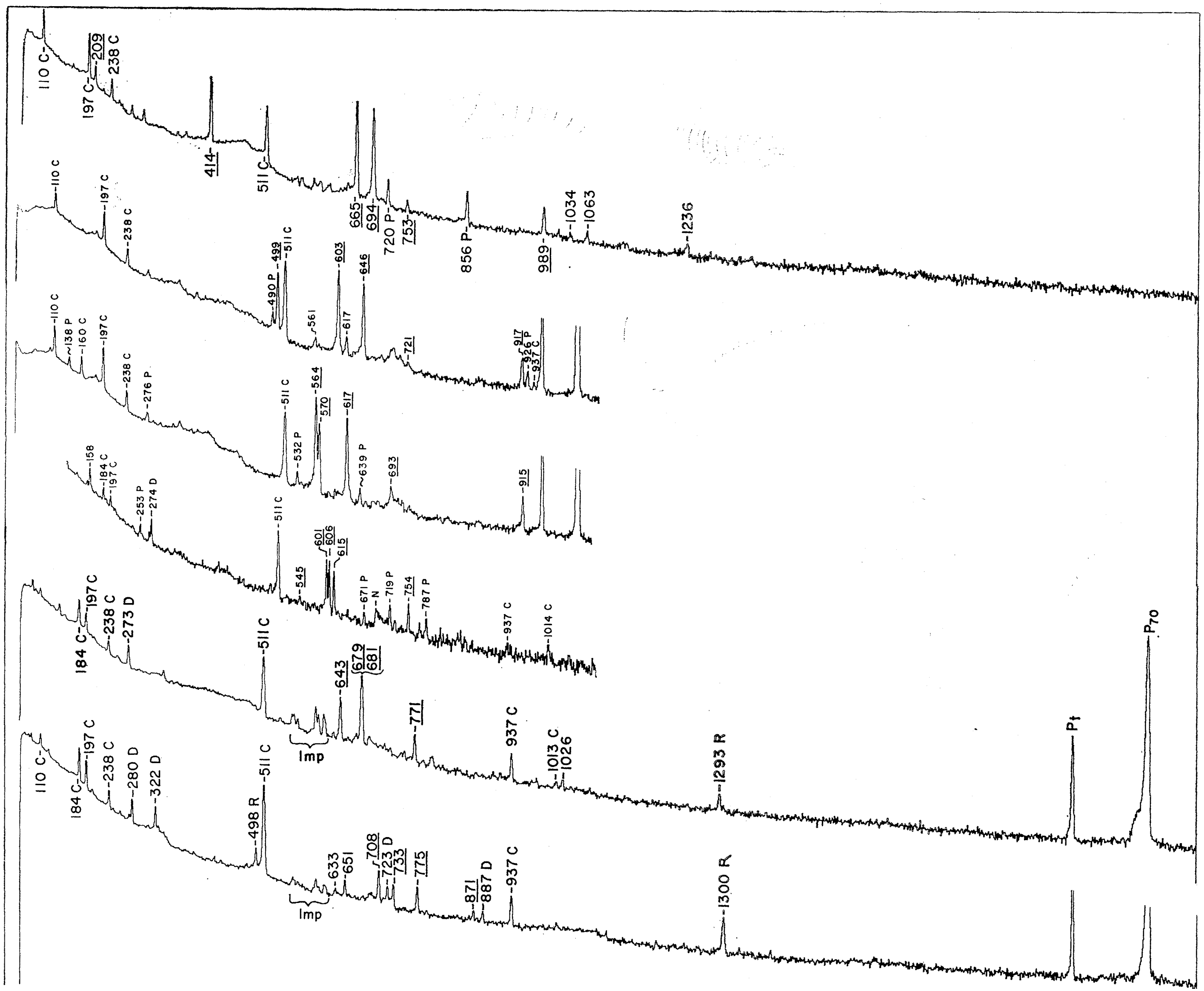

FIG. 3. γ-ray spectra averaged over all time. From the top they are 25-MeV $(\alpha, 2n)$ ^{126}Te, 28-MeV $(\alpha, 2n)$ ^{124}Te, 28-MeV $(\alpha, 2n)$ ^{122}Te, 61-MeV $(\alpha, 4n)$ ^{118}Te, 36-MeV $(\alpha, 2n)$ ^{116}Te, and 36-MeV $(\alpha, 2n)$ ^{114}Te. The pulser peaks P_t and P_{70}, used for dead-time correction, have been truncated in some cases to save space. Peaks labeled P have only prompt components, and D denotes peaks delayed in Fig. 2. Impurities are denoted Imp.

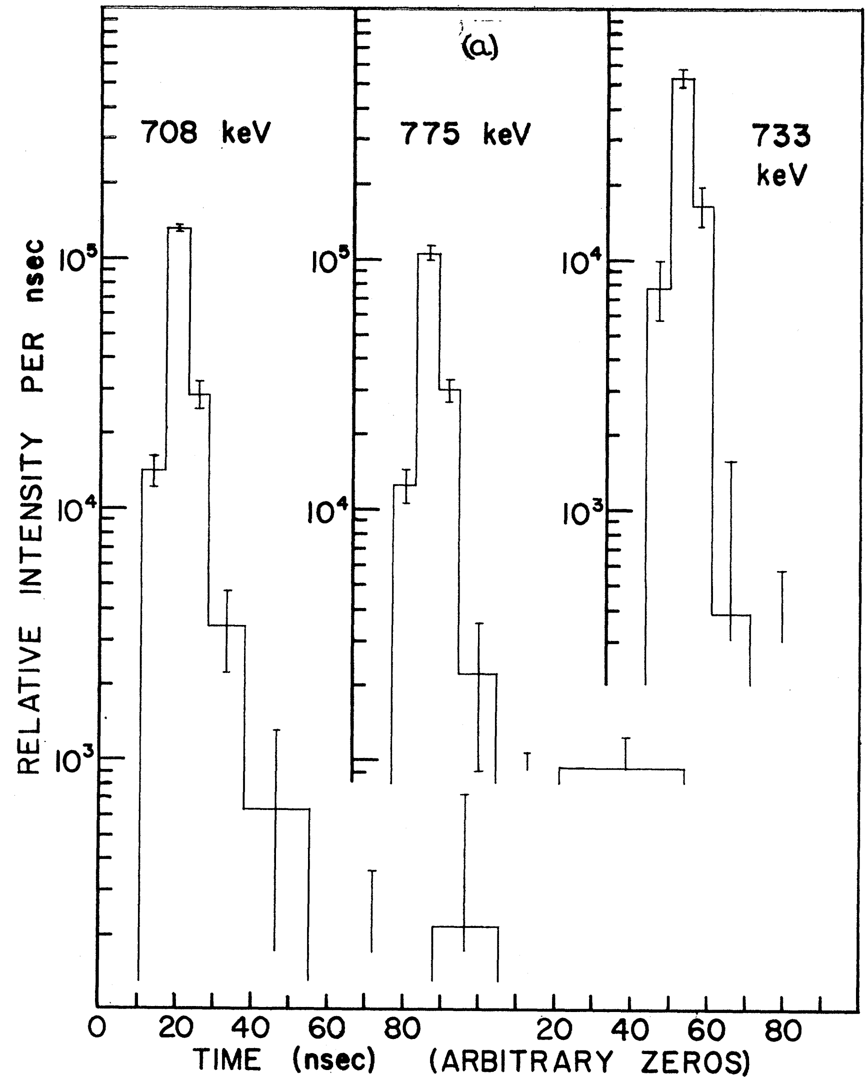

FIG. 4. (a) Examples of time distributions of transitions in 36-MeV (α, $2n$) ^{114}Te. This is typical of all transitions in Fig. 7 except those in the ground-state band of ^{126}Te. (b) Time distributions of all transitions in ^{126}Te in Fig. 7 except the 753-keV transition, which is prompt. Only the 209-keV transition has no prompt component.

discrepancy for ^{126}Te at 28.5 MeV is caused only by the prompt component of the $4^+ \to 2^+$. It is believed that there is an additional prompt (only) transition at about 694 keV which is rapidly becoming more intense with increasing E_α.

V. LEVEL ASSIGNMENTS

The level assignments from these data are in Fig. 7. Levels from other works will be discussed separately if they were published after the closing date (March, 1966) of Lederer *et al.*[15]

The solid curves for the angular distributions of Fig. 5 for $^{114-124}$Te and the dashed curves for ^{126}Te have all been calculated[16] from the assigned level spins J in Fig. 7, the experimental transition intensities, and a Gaussian width σ_J for the side-feeding population of magnetic substates of

$$\sigma_J = 1.0 + 0.15J. \quad (9)$$

The fit is good for all but ^{126}Te. The solid curves for ^{126}Te in Fig. 5 are calculated from

$$\sigma_J = 1.8 + 0.1J. \quad (10)$$

In both cases it has been assumed, somewhat arbitrarily, that the 209-keV γ ray in ^{126}Te originated from a level of $J = 10$, with a large effective σ of 6.0.

A. Levels in ^{126}Te

The 13-nsec component in the 209-, 989-, 414-, 694-, and 665-keV transitions is a characteristic signature of a cascade. The 209-keV transition has no measurable prompt component; thus it is from the isomeric level. The qualitative features of its angular distribution are characteristic of stretched quadrupole,

[16] J. E. Draper and R. M. Lieder (to be published).

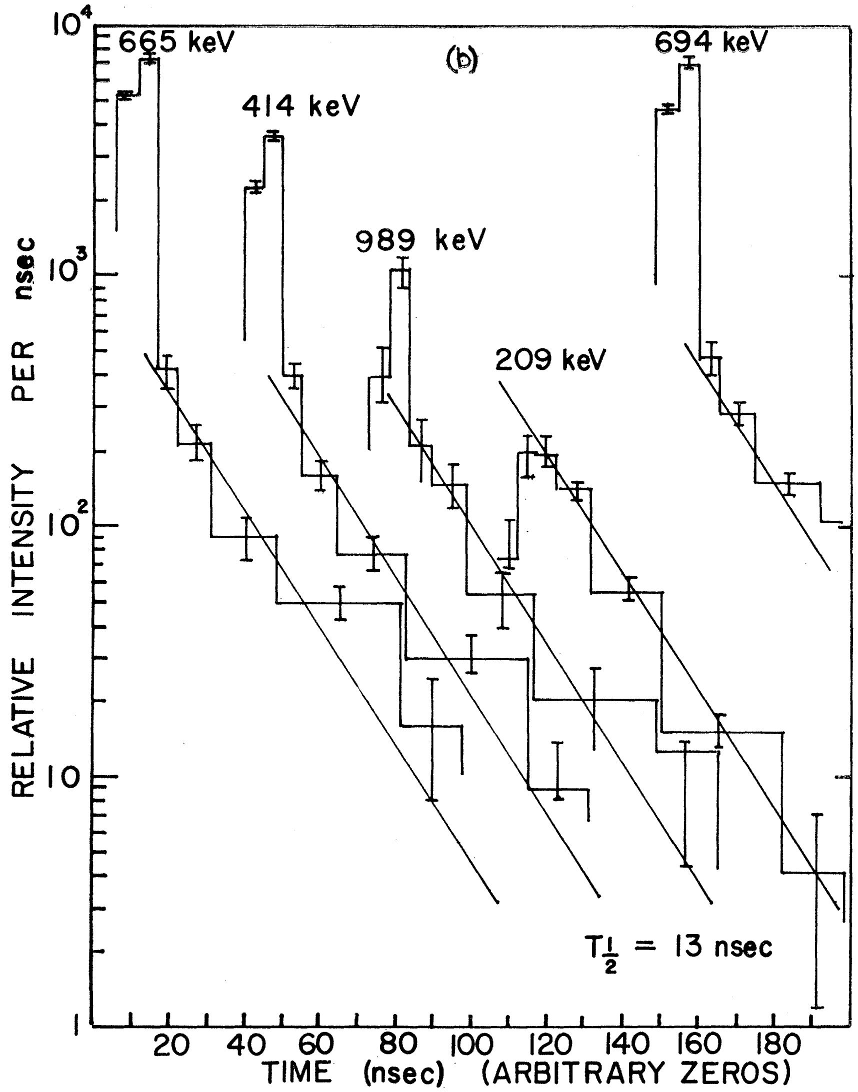

FIG. 4. (*Continued*).

$J(1)J$, or octupole transitions, but they are incompatible with $J(2)J$ for $J\neq 1$, $J(2)J-1$, and stretched dipole. A quadrupole transition would have an electron conversion coefficient (0.10 for $E2$ and 0.36 for $M2$) to bring the transition intensities (Table I) of the 13-nsec components of the 209-, 989-, 414-, 694-, and 665-keV transitions to equality, within the uncertainties, as required when they are in cascade. The ordering of the transitions is dictated by increase in the *prompt* intensities down the cascade because of side feeding. The uncertainties in the intensities of the 665- and 694-keV transitions introduce ambiguity as to their order. However, Pramila *et al.*[17] with (p, p') locate the first 2^+ state at 670 ± 5 keV.

The assignment as stretched $E2$ for the 989-, 414-, 694-, and 665-keV transitions is based on the angular distributions. The systematic empirical dominance of stretched $E2$ transitions in the now large body of experimental results from (α, xn) reactions motivates cautious rejection of $J(1)J$ and octupole transitions which have angular distributions qualitatively similar to that of stretched $E2$. The assignment of stretched $E2$ transitions as $J(2)J-2$ rather than occasionally $J(2)J+2$ is based on the experimental absence of crossover transitions and on the systematics.

TABLE I. Transition intensities in ^{126}Te.

E_γ (keV)	I^{prompt}	$I^{13\text{ nsec}}$	Assignment
665	0.90 ± 0.1	0.11 ± 0.015	$2^+\to0^+$
694	0.87 ± 0.1	0.10 ± 0.015	$4^+\to2^+$
414	0.35 ± 0.03	0.10 ± 0.015	$6^+\to4^+$
989	0.10 ± 0.015	0.08 ± 0.015	$8^+\to6^+$
209	<0.01	0.08 ± 0.015[a]	$\cdots\to8^+$ [b]

[a] Assuming an $E2$ conversion coefficient.
[b] See text for level assignment.

[17] G. C. Pramila, R. Moddleton, T. Tamura, and G. R. Satchler, Nucl. Phys. **61**, 448 (1965).

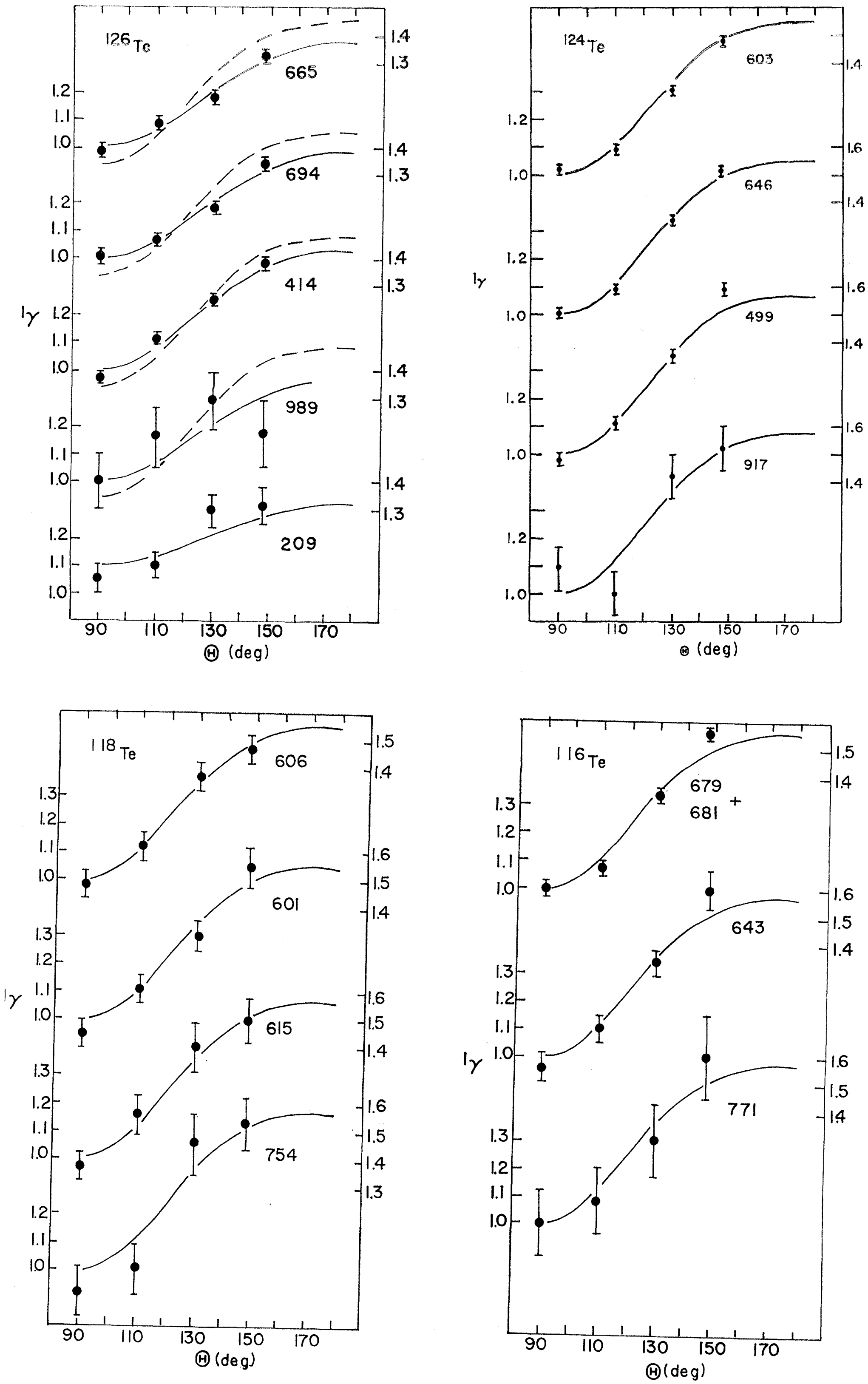

FIG. 5. Angular distribution data. The calculated solid and dashed curves are explained in the text. The angle θ (deg) is the same as in Eq. (7).

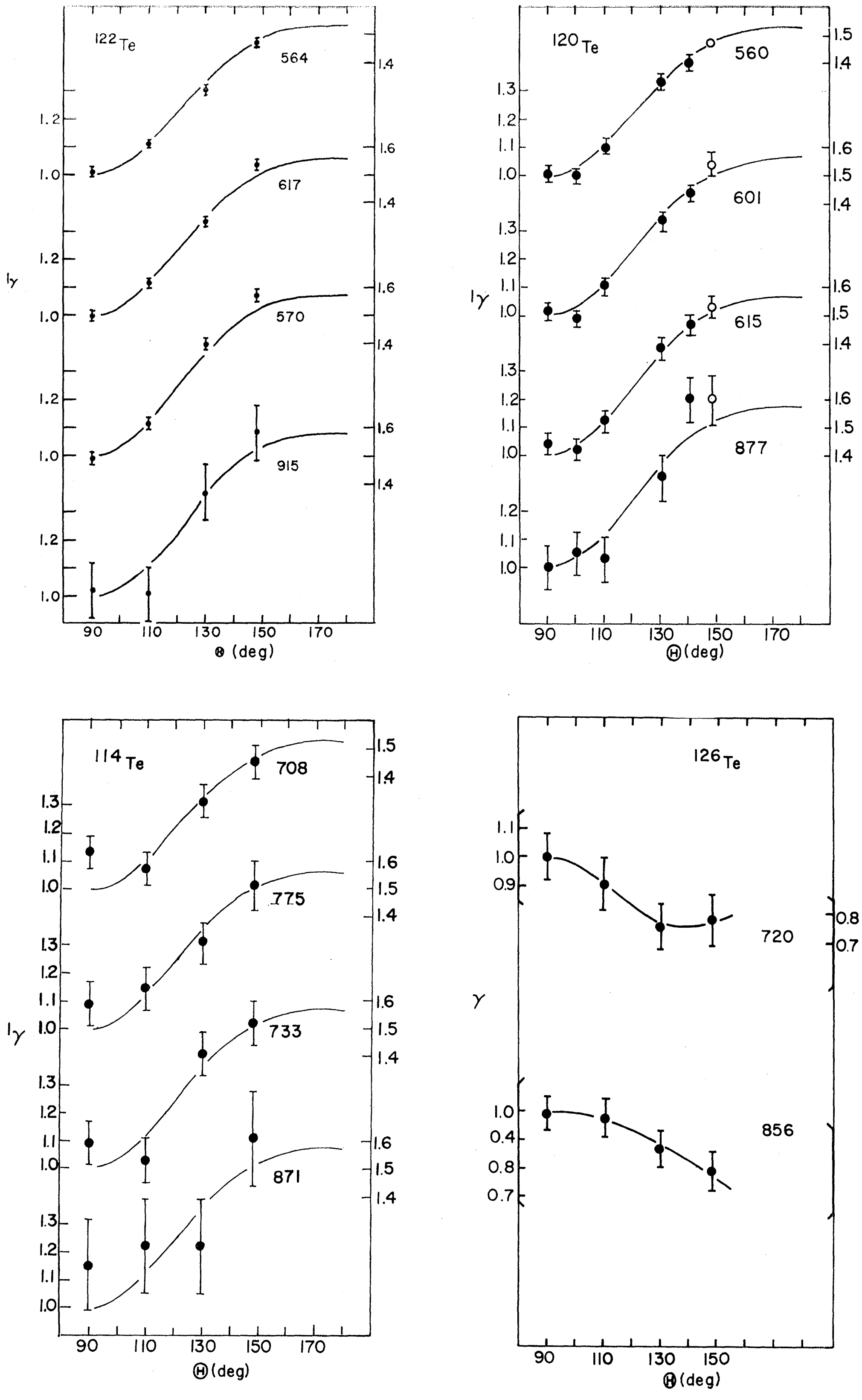

FIG. 5. (*Continued*).

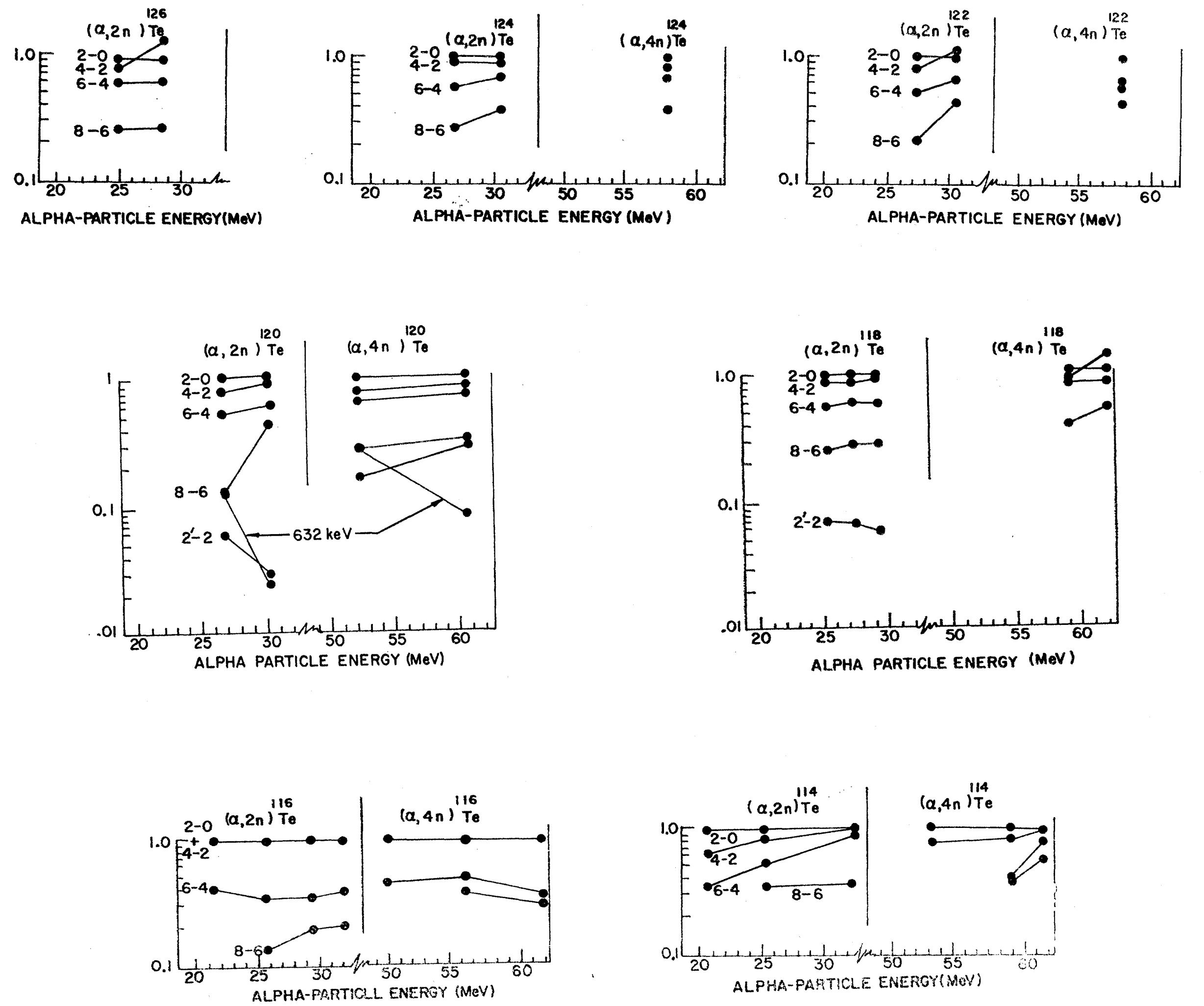

FIG. 6. Relative transition intensities versus α-particle energies. The curve for the 209-keV transition in ^{126}Te is nearly parallel to that for the 8–6 transition and was omitted inadvertently.

The 13-nsec 209-keV transition probability is ~4 Weisskopf units if it is pure $E2$. The typical collective enhancement factor for 2→0 transitions of this energy is ~70. If it is $M2$, it is enhanced by a factor ~150; if $M1$, it is inhibited by a factor ~10^4; and if $E1$, by a factor ~10^6. If the isomeric level is another spin-8 level, then the angular distribution of the 209-keV transition requires that it be nearly pure dipole. If the level is spin-9, then the angular distribution shows that the transition cannot be pure dipole nor pure quadrupole but must be roughly equal proportions of each.

The $2^{+\prime}\to 2^+$ assignment of the 753-keV γ ray is assisted by the β-decay work of Lagrange *et al.*,[18] who find a 755-keV $2^{+\prime}\to 2^+$ with the $2^{+\prime}\to 0^+$ crossover only 0.07 times as intense. The angular distribution of the very weak 753-keV γ ray is nearly isotropic, so it contains substantially more $E2$ than $M1$.

The transitions in ^{126}Te in Fig. 7 below the 6^+ level compare reasonably well with the dashed levels and transitions of Bergström *et al.*[6] However, there are energy discrepancies up to 16 keV for the $2^{+\prime}$ level. The 2^+, (4^+), and 2^+ levels in Lederer *et al.*[15] at 0.667, 1.36 and 1.42 MeV, respectively, are not inconsistent with our results.

B. Levels in ^{124}Te

The prominent transitions in ^{124}Te are prompt ($\lesssim$3 nsec). The energies, intensities, angular distributions, and excitation functions were used for the assignment of levels in Fig. 7. The 926-keV transition is not assigned. Its angular distribution is nearly isotropic unlike that of the 917-keV transition.

The assignment of the weak 721-keV transition as $2^{+\prime}\to 2^+$ is based on the β-decay work of Lagrange *et al.*,[18] who found 723 keV. They found the $2^{+\prime}\to 0^+$ to be only 0.15 times as intense as the $2^{+\prime}\to 2^+$, so that we could not observe the former. The intensity of the 721-keV transition is too small for a meaningful angular distribution.

[18] J.-M. Lagrange, G. Albouy, L. Marcus, M. Pautrat, H. Sergolle, and O. Rahmouni, Ann. Phys. (Paris) 2, 141 (1967).

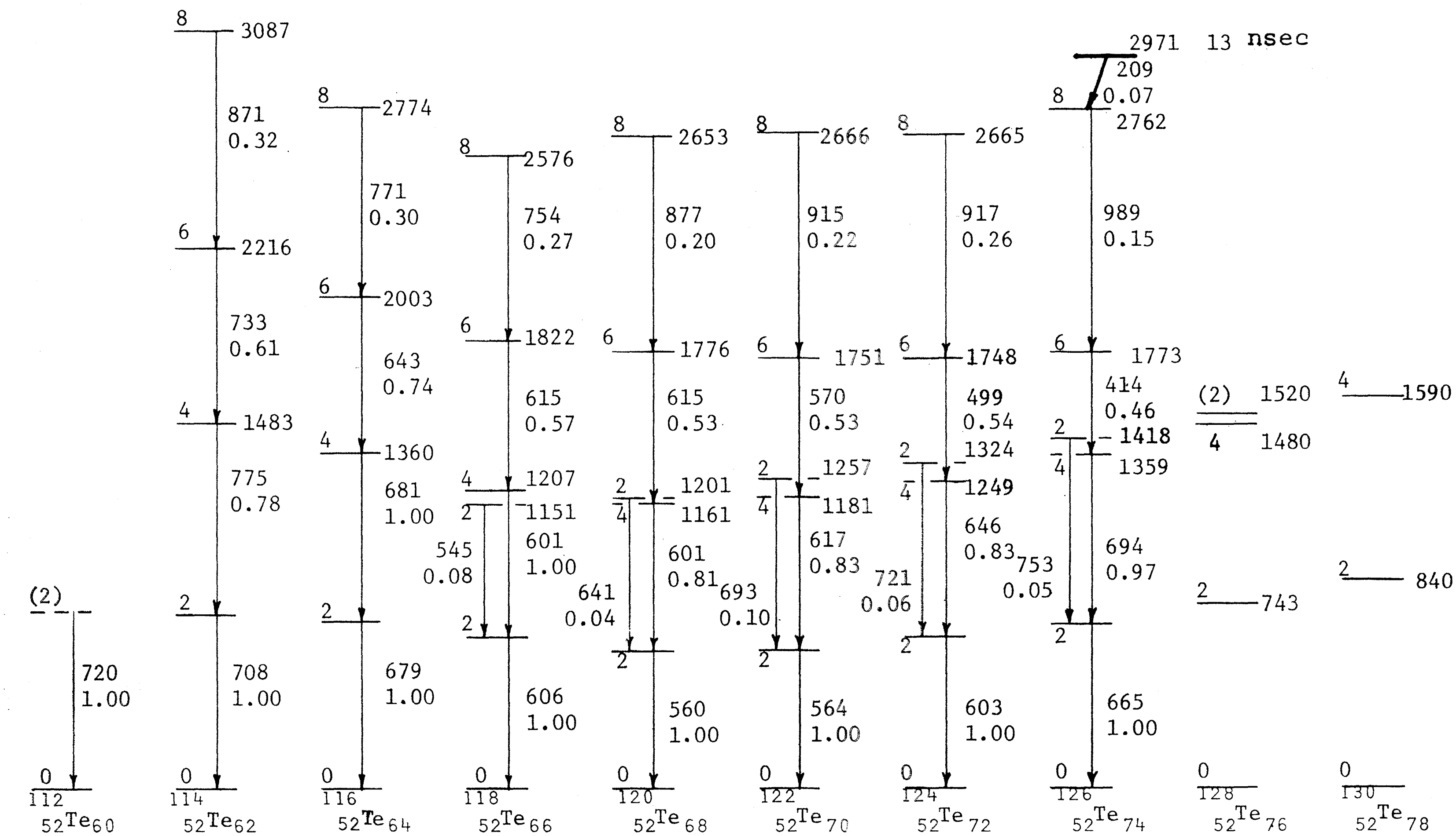

FIG. 7. Energy levels of Te isotopes. Arrows denote transitions observed and identified in this work. Levels in ^{128}Te and ^{130}Te from other laboratories are included for comparison.

Our results are consistent with the 603-keV 2^+ level and the 1248-keV (4^+) level reported by Lagrange *et al.*[18] The results of Bergström *et al.*[6] are consistent with ours for transitions below the 6^+ level. The 2^+, (4^+), $2^{+\prime}$, and (6^+) levels in Lederer *et al.*[15] are consistent with ours. There is no correspondence with the 720-keV $6^+\rightarrow4^+$ assignment of Ref. 5.

C. Levels in ^{122}Te

The prominent transitions of interest are only prompt ($\lesssim 3$ nsec). The intensities, angular distributions, and excitation functions give the level assignments of Fig. 7. The 693-keV line is partially obscured by the neutron peak, so that no angular distribution was possible. It is assigned as $2^{+\prime}\rightarrow2^+$ on the basis of the assignment of the 693-keV line from Lagrange *et al.*[18] and the 693-keV line from Spejewski *et al.*[19] in which the $2^{+\prime}\rightarrow0^+$ was only 0.16 times as intense as the $2^{+\prime}\rightarrow2^+$. The results of Bergström *et al.*[6] are in good agreement with ours below 6^+. The levels in Ref. 15 labeled 2^+, (4^+), and 2^+ at 0.564, 1.17, and 1.25 MeV, respectively, are not inconsistent with ours. There is reasonable agreement with the 2^+, 4^+, and $2^{+\prime}$ levels of Ref. 4 and the 2^+ and 4^+ levels of Ref. 5.

D. Levels in ^{120}Te

The prominent transitions of interest are all prompt ($\lesssim 3$ nsec) and are assigned by the method above. The $2^{+\prime}\rightarrow2^+$ assignment of the weak 641-keV line is also based on the same assignment of the 640-keV line of Ladenbauer-Bellis and Bakhru[20] and the 641-keV line of Lagrange *et al.*[18] It was too weak for a useful angular distribution. This $2^{+\prime}\rightarrow2^+$ assignment was given to the 632-keV line of Fig. 2(b) by Bergström *et al.*,[6] but Fig. 6 shows that its excitation function is unsatisfactory for this assignment.

The energy of our $6^+\rightarrow4^+$ is typographically inverted in Ref. 7. The levels in Fig. 7 are consistent with the 2^+, (4^+), and 2^+ levels of Lagrange *et al.*[18] at 561, 1162, and 1202 keV, respectively, and the 2^+, (3, 4), 2^+, and $(4^+, 5, 6)$ levels of Ladenbauer-Bellis and Bakhru[20] at 560, 1160, 1200, and 1772 keV, respectively. Agreement with the 2^+ and 4^+ levels of Refs. 4 and 5 is satisfactory.

E. Levels in ^{118}Te

The prominent transitions of interest are all prompt ($\gtrsim 3$ nsec) and are assigned by the method above. The $2^{+\prime}\rightarrow2^+$ assignment of the weak 545-keV line is also based on the 542-keV result of Ladenbauer-Bellis and Bakhru[20] and the 544.8-keV result of Spejewski *et al.*[19] The line was too weak for a useful measurement of angular distribution. The 601- and 606-keV lines are of nearly the same intensity, so that their order is uncertain. Figure 6 shows the 601-keV line to be slightly less intense. The contributions to the 601- and 615-keV lines from the ^{118}Sn impurity in the target are less than 4%, based on the absence of a 560-keV line in Fig. 3. The placement of the first 2^+ state at 606 keV is confirmed by the coincidence data from radioactivity by Spejewski *et al.*,[19] who find that the 545-keV line is in coincidence with the 606 but not with the 601-keV line. Possible candidates for the $8^+\rightarrow6^+$ are the prompt 754-, 787-, and 850-keV transitions. However, the 850-keV line is very weak (Fig. 3) in $(\alpha, 4n)$, so it is rejected. The angular distributions and excitation functions of the 754- and 787-keV lines are both satisfactory for $8^+\rightarrow6^+$. The 754-keV line is selected for $8^+\rightarrow6^+$ primarily because it is 45% more intense than the 787-keV line and better fits the systematics of intensities in Fig. 7. Our results are in agreement below 6^+ with Bergström *et al.*[6] They are not in agreement with the results of Lagrange *et al.*,[18] who have the (4^+) and 2^+ levels at 1151 and 1206 keV, respectively. They are not in agreement with the 610-keV $4^+\rightarrow2^+$ of Ref. 4 nor the 558-keV for that transition in Ref. 5.

F. Levels in ^{116}Te

The prominent transitions of interest are prompt ($\lesssim 3$ nsec) except for the 273-keV line, and are assigned by the method above. The peak in Fig. 3 labeled 679, 681 keV was earlier thought to be a single transition. This is in error in Ref. 7. However, it would have had more than twice the intensity (relative to the other transitions in ^{116}Te) compared to the systematics of the other isotopes in Fig. 7. This was further substantiated by recent data from Stockholm[21] obtained with a coaxial Ge(Li) detector in which the two peaks were partially resolved. The doublet in our data was confirmed by computer analysis of our line shapes at both 90° and 148°, resulting in $I_{681}/I_{679}=1.0\pm0.1$ with an energy separation of 1.7 ± 0.1 keV.

The relative order of the 679-keV and 681-keV transitions in Fig. 7 is arbitrary.

Recent tentative results[19] on β decay of ^{116}I produced by spallation reveal none of the transitions seen here. No other information is available from radioactive decay. There is no correspondence with the 607-keV $2^+\rightarrow0^+$ transition in Ref. 5.

G. Levels in ^{114}Te

The transitions of interest in ^{114}Te in Fig. 2(g) are all prompt ($\lesssim 3$ nsec). The levels are shown in Fig. 7. The 498-keV line in Fig. 3 has no measurable prompt or short-lived ($\lesssim$200-nsec) component and also appears in a spectrum taken shortly after extinguishing the cyclotron beam. It is probably from the first excited state[15] in ^{115}Sn from β^+ decay of ^{115}Te through ^{115}Sb. This could also account for the delayed component of the 723-keV line as being from the first excited state[15]

[19] E. H. Spejewski, P. K. Hopke, and F. W. Loeser, Jr. (private communication).

[20] I.-M. Ladenbauer-Bellis and H. Bakhru, Phys. Rev. **175**, 1507 (1968).

[21] A. Kerek (private communication).

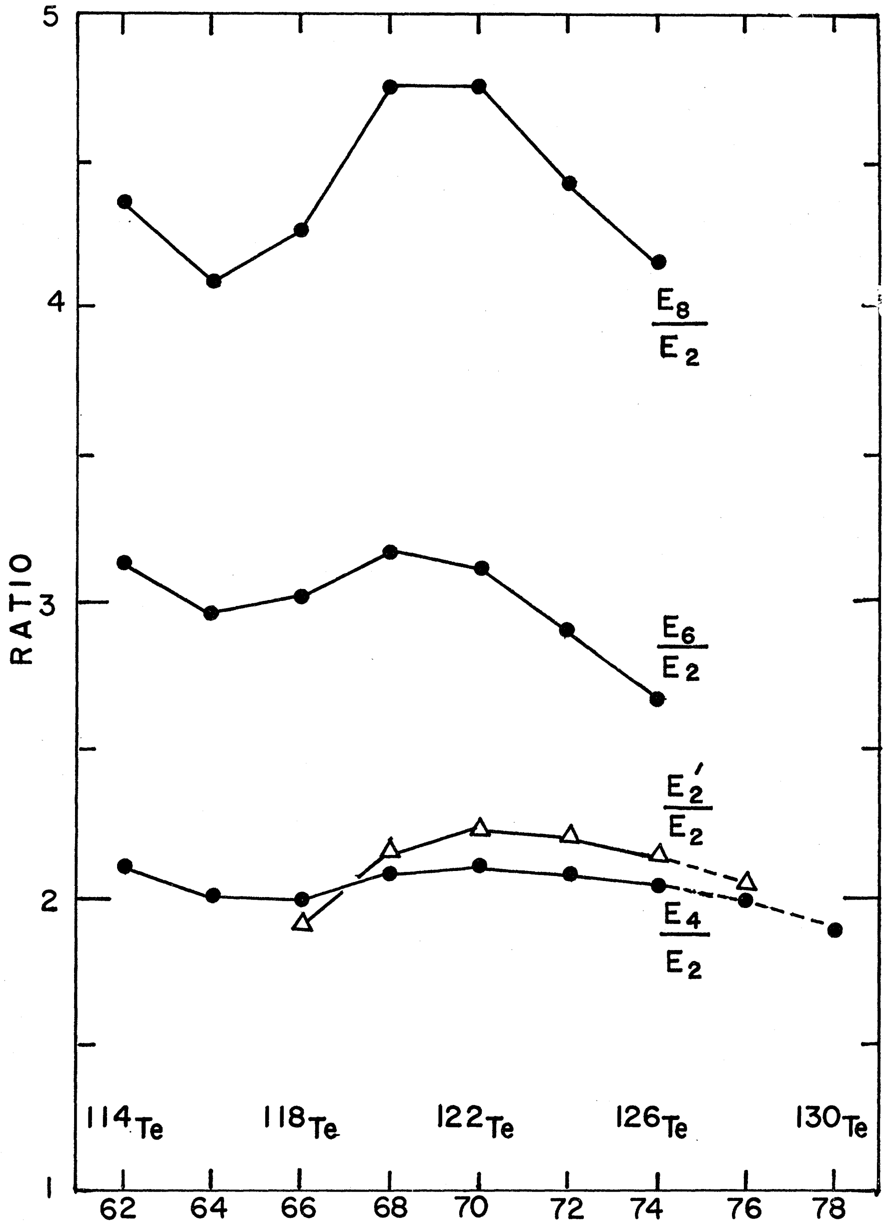

FIG. 8. Ratios of level energies from Fig. 7.

of ^{115}Sb at 0.72 MeV, although it also has a prompt component which would then require (α, p).

Our results for ^{114}Te are in disagreement with the preliminary results of Bergström *et al.*,[22] who assigned transitions of 511, 497.5, and 280 keV as $2^+ \rightarrow 0^+$, $4^+ \rightarrow 2^+$, and $6^+ \rightarrow 4^+$, respectively. This would have constituted a substantial break in the level energy systematics at neutron number 64 and was thought[22,23] to be like the Sn isotopes[23] in this respect. This, in turn would render less satisfactory the promising calculations of Marumori *et al.*[24] However, our time analysis of the 280- and 498-keV lines shows no evidence of a prompt component. The prompt component of our 511-keV line is similar to that for other isotopes and originates in pair production by prompt energetic gammas. Their more recent data and interpretation[21] are in agreement with our results.

H. Levels in ^{112}Te

These transitions could only be produced by (α, $4n$) since ^{112}Sn is the lightest stable Sn isotope. For this

[22] I. Bergström, C. J. Herrlander, A. Kerek, and A. Luukko, J. Phys. Soc. Japan Suppl. **24**, 659 (1968).

[23] T. Yamazaki, G. T. Ewan, and S. G. Prussin, Phys. Rev. Letters **20**, 1376 (1968).

[24] T. Marumori, M. Yamamura, Y. Shono, A. Tokunaga, and Y. Miyanishi, J. Phys. Soc. Japan Suppl. **24**, 581 (1968); T. Marumori, M. Yamamura, Y. Miyanishi, and N. Nishiyama, Progr. Theoret. Phys. (Kyoto) Suppl. **179**, Extra No. (1968).

reaction, Eq. (8) gives $E_\alpha^{\rm opt}=71$ MeV. The γ-ray spectra from such high-energy α particles are not as clear as for $(\alpha, 2n)$. Spectra taken with 70-MeV α particles and 1.5-MeV full-scale γ energy showed prompt 720- and 1060-keV lines. No angular distributions nor excitation functions were possible. However, on the basis of the systematics of energy levels and $(\alpha, 4n)$ yields, the 720-keV line is assigned to the first 2^+ level in ^{112}Te. No other investigations of ^{112}Te are known.

VI. DISCUSSION

The beautiful systematics of energies, spins, and transition intensities exhibited in Fig. 7 for these most prominent transitions is self-evident. It is remarkable that the most prominent lines in these $(\alpha, 2n)$ and $(\alpha, 4n)$ γ-ray spectra of even-even vibrators should involve only the level sequence 8^+, 6^+, 4^+, 2^+, and 0^+. In more rigid nuclei with large ground-state deformations, this sequence is a more familiar quasirotational ground-state band. There is no marked evidence of the effect of the intermediate shell closure at $N=64$, although this closure dominated the characteristics of the Sn isotopes, only two protons away, and Te was then thought to be a similar case.[22,23]

Figure 8 shows the ratios of level energies for various levels and isotopes. Departures from integer ratios are substantial in the higher levels. The ground-state deformations calculated by Marshalek *et al.*[3] for the Te nuclei lie on a bell-shaped curve with a broad maximum at $A=116$ and half-maxima at $A=106$ and 124. This curve is displaced about 4–6 neutrons lower than the center of the pattern of the first 2^+ levels in Fig. 7.

Ward, Stephens, and Diamond[25] have reported a systematic search for isomers with lifetimes >0.1 msec in isotones with 74 neutrons. They found evidence for 8^- or 9^- isomers in ^{134}Nd, ^{132}Ce, and ^{130}Ba, shown in Fig. 9, with no evidence for such lifetimes in ^{126}Te or ^{128}Xe. It is not clear that the microscopic origin of the 13-nsec levels in ^{126}Te is similar to that of those isomers.

Let us return briefly to the question why the most prominent transitions following these (α, xn) reactions producing "vibrator" nuclei are those involving an $8^+\to6^+\to4^+\to2^+\to0^+$ sequence of levels, although there are many other levels in the energy region. The spin pattern is strongly suggestive of a rotor. If one uses the most probably angular momenta shown in Fig. 1 and calculates the excitation energy just after neutron emission due to collective rotation with a moment of inertia $\frac{1}{3}$ [for $(\alpha, 2n)$] to $\frac{1}{2}$ [for $(\alpha, 4n)$] that of a rigid rotor, the result is that about $\frac{2}{3}$ of the total excitation energy is in kinetic energy of rotation. It would then appear that the strongly excited levels at the upper edge of Fig. 7 would have a significantly rotational character. On the other hand, it might be argued that

[25] D. Ward, F. S. Stephens, and R. M. Diamond, Nuclear Chemistry Division Annual Report No. UCRL-18667, p. 54, 1968 (unpublished).

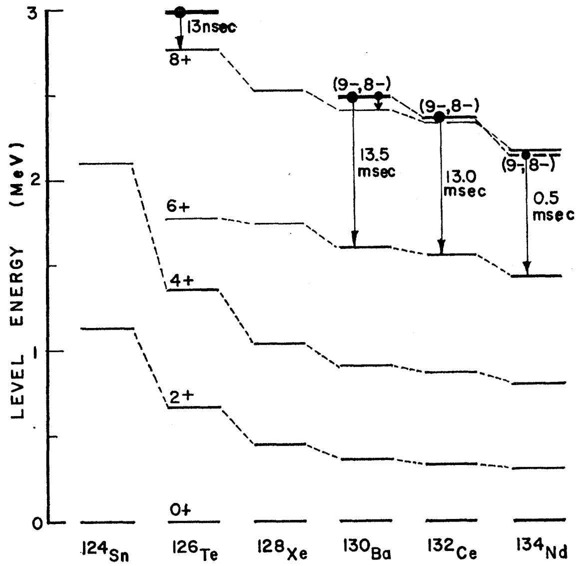

FIG. 9. Ground-state band and isomeric levels in nuclei with $N=74$. The ^{124}Sn levels are from Ref. 18. The ^{126}Te levels are from this work. The remainder are from Ref. 20, except the 8^+ level in ^{128}Xe from Ref. 6.

the levels in Fig. 7 are merely the highest-spin members of each vibrational multiplet, i.e., they are the YRAST levels.[8,10] If that is the only consideration, then it is not obvious that the next lower-spin members of each vibrational multiplet would not also be fairly strongly excited. Since there are still some unassigned prompt, weak transitions in the data this can not be ruled out. In part, both of the effects above may be important as discussed in the next paragraph.

Marumori *et al.*[24] have presented a unified microscopic theory of vibrational and rotational motion in even-even nuclei. This extended RPA theory appears to describe only the levels $\cdots 8^+$, 6^+, 4^+, 2^+, 0^+ which dominate the present (α, xn) experimental spectra. For particles restricted to one j shell, the ratios of the energies of each of the levels in the band to the energy of the 2^+ state depends on only one parameter. It remains to be seen how successfully such calculations for Te would match the results in Fig. 7, although most of the qualitative features are correct. It appears that there might be some difficulty in matching the relatively small energy of the $6^+\to4^+$ transition in the heavier isotopes.

An empirical analysis[2] of experimental results on quasirotational ground-state bands including $\sim$355 transitions in $\sim$88 even-even nuclei of $A>96$ shows that the trend of the level patterns for high spins gives $\mathcal{I}_{16}/\mathcal{I}_{\rm rigid}$ within 40% of 0.42 $\mathcal{I}_{\rm rigid}$ in all cases. Here $\mathcal{I}_{16}$ is the moment of inertia for spin 16 and $\mathcal{I}_{\rm rigid}$ is the rigid moment of inertia. This is the basis for the use of $\frac{1}{3}$ to $\frac{1}{2}$ $\mathcal{I}_{\rm rigid}$ in the previous paragraph. This empirical analysis reflects the same sort of simplicity of structure as is contained in the results of Marumori *et al.*[24] The systematics displayed in Figs. 7 and 9 for isotopes and isotones are consistent with this simplicity. The simple empirical mathematical equation[2] for the level energies produces a pattern of level energies approaching $I(I+1)$ for hard nuclei (between major shell closures) and produces a nearly constant spacing of levels for soft nuclei (near major shell closures). This empirical result is put on a firm theoretical microscopic basis by Marumori *et al.*[24]

The theoretical analysis of the levels of Te by Alaga *et al.*[26] as two protons coupled to a harmonic vibrator gives reasonable results for the first approximately two excited states in the bands of Fig. 7. The protons are taken as interacting through a pairing force and are coupled to the harmonic vibrator with a particle-surface interaction. There are several adjustable parameters. However, that theoretical approach does not emphasize only those levels which dominate these (α, xn) experimental results, in contrast with the approach of Marumori *et al.*[24]

Note added in proof. After this work was submitted, the work of Luukko *et al.* [Nucl. Phys. **A135**, 49 (1969)] was published. Their Fig. 3 matches our results quite well, although they did not assign 8+ levels in ^{120,122,124,126}Te, and only tentatively in ^{118}Te; they had only tentative 2+, 4+, and 6+ levels in ^{126}Te, and did not report the 13-nsec component of the five transitions in ^{126}Te.

ACKNOWLEDGMENTS

We are indebted to Dr. G. L. Smith, who participated in all phases of the development of these experiments. We are also indebted to D. G. McCauley, who made several specific contributions.

APPENDIX

Define $r_\gamma(t)$ as the total γ counting rate for all pulses presented to the analyzer at time t and approximate that most of it is not from delayed transitions. Define $l(t)$ as the probability that the analyzer is live at time t. Then for the ith γ transition we must determine the live time ratio L_i in order to correct for dead time. This is defined as

$$L_i = \int (r_i l dt / r_i dt) = \text{counts stored/counts presented}, \tag{A1}$$

where the integrals extend over the run. The live probability is

$$l(t) = \exp\left(-\int_{t-T}^{t} r_\gamma(\tau)\, d\tau\right), \tag{A2}$$

where T is the analyzer dead-time interval.

The ratio L_i is evidently dependent on the time structure of the cyclotron beam and on the half-life of the ith transition. For a prompt transition (half-life $\ll T$), L_i can be measured by mixing into the analyzer input the output of a pulser triggered by the monitor Ge(Li) counter. Defining this triggered pulser rate as $r_{\mathrm{trig}}(t)$, then since r_{trig}/r_i is constant for a prompt transition, we have

$$L_{\mathrm{trig}} = L_i, \tag{A3}$$

and the dead-time correction is accurately made with the triggered pulser.

The other extreme case for L_i is obtained from a transition of half-life $\gg$ any characteristic time of beam structure. This can be simulated by mixing at the analyzer input pulses from a fixed frequency pulser asynchronous with 60 Hz. We used a 70-Hz pulser and the resulting L_{70} is the largest L_i obtainable. Evidently a pulser synchronous with the beam structure is useless. For the analysis above the assumption has been made that both pulsers have rates $\ll r_\gamma$.

In summary,

$$L_{\mathrm{trig}} \lesssim L_i \lesssim L_{70}. \tag{A4}$$

For one set of our data $L_{70}/L_{\mathrm{trig}} = 4$, whereas useful angular distributions require a knowledge of L_i to a few percent. In addition, uncorrected relative intensities of short-lived and long-lived transitions within a given spectrum are incorrect.

[26] G. Alaga, F. Krmpotic, and V. Lopac, Zagreb Report No. I.R.B.-TP-2 (unpublished).